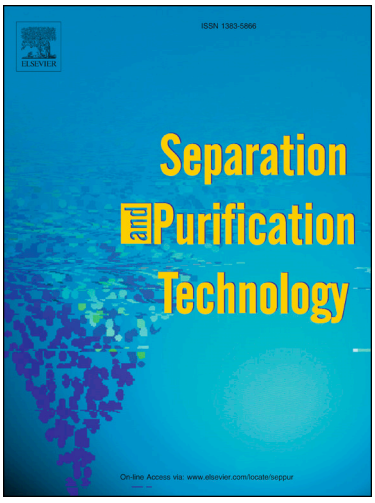

Electrocoagulation as a green technology for phosphate removal from River water

Khalid S. Hashim, Rafid Al Khaddar, Nisreen Jasim, Andy Shaw, David Phipps, P. Kot, Montserrat Ortoneda Pedrola, Ali W. Alattabi, Muhammad Abdulredha, Reham Alawsh

PII: S1383-5866(18)31326-1
DOI: https://doi.org/10.1016/j.seppur.2018.07.056
Reference: SEPPUR 14787

To appear in: *Separation and Purification Technology*

Received Date: 18 April 2018
Revised Date: 22 June 2018
Accepted Date: 22 July 2018

Please cite this article as: K.S. Hashim, R. Al Khaddar, N. Jasim, A. Shaw, D. Phipps, P. Kot, M. Ortoneda Pedrola, A.W. Alattabi, M. Abdulredha, R. Alawsh, Electrocoagulation as a green technology for phosphate removal from River water, *Separation and Purification Technology* (2018), doi: https://doi.org/10.1016/j.seppur.2018.07.056

Electrocoagulation as a green technology for phosphate removal from River water

Khalid S. Hashim[a, b*], Rafid Al Khaddar[a], Nisreen Jasim[b], Andy Shaw[a], David Phipps[a], P. Kot[a], Montserrat Ortoneda Pedrola[a], Ali W. Alattabi[a,c], Muhammad Abdulredha[a,d], Reham Alawsh[b]

[*]*Corresponding author: Khalid Hashim, assist. Prof, e-mail: k.s.hashim@ljmu.ac.uk*
[a] *School of Civil Engineering, Liverpool John Moores University, Liverpool, UK.*
[b] *Department of Environment Engineering, University of Babylon, Babylon, Iraq.*
[c] *Department of Environment Engineering, University of Wasit, Wasit, Iraq.*
[d] *Department of Environment Engineering, University of Karbala, Iraq.*

Abstract

The current study investigates the removal of phosphate from water using a new baffle plates aluminium-based electrochemical cell (PBPR) taking consideration the influence of key operating parameters. This new cell utilises perforated baffle plates as a water mixer rather than magnetic stirrers that require extra power to work. As this unit is new, a comprehensive study has been carried to assess it performance. This study also includes preliminary estimates of the reactor's operating costs, the amount of H_2 gas produced and the yieldable energy from it. SEM (scanning electron microscope) was used to investigate the influence of the electrocoagulation process on the morphology of the surface of aluminium electrodes, and an empirical model developed to reproduce the phosphate removal process.

The results showed that 99% of phosphate was removed within 60 minutes of electrolysis at an initial pH (ipH) of 6, inter-electrode distance (ID) of 0.5 cm, current density (J) of 6 mA/cm^2, initial concentration of phosphate (IC) of 100 mg/L, and minimum operating cost of 0.503 US \$/m^3. The electrochemical cell produced enough H_2 gas to generate 4.34 kWh/m^3 of power.

Statistically, it was proved that the influence of the operating parameters on phosphate removal could be modelled with an R^2 of 0.882, the influence of these operating parameters on phosphate removal following the order: $t > J > IC > ipH > ID$. Finally, SEM images showed that after several electrolysing runs, the Al anode became rough and nonuniform which could be related to the production of aluminium hydroxides.

Keywords: Electrocoagulation; phosphate; multiple regression model; hydrogen gas; SEM; operating cost.

1. Introduction

Phosphorus is a non-metallic element with the atomic number 15 and an atomic mass of 30.974 amu (Fadiran *et al.*, 2008). It is an important nutrient for the growth of organisms (Barca *et al.*, 2012) and it is not categorised as a harmful or toxic element for mankind at low concentrations (Attour *et al.*, 2014). Phosphorus occurs in the aquatic environment as dissolved phosphate forms such as orthophosphates, polyphosphates and organic phosphate (Behbahani *et al.*, 2011; Lacasa *et al.*, 2011). However, the most thermo-dynamically stable and dominant form of phosphate is orthophosphate, which represents about 50% of the total amount of phosphate, other forms comprising the remaining 50% (Fadiran *et al.*, 2008; Sibley, 2013; Strileski, 2013). Due to the instability of polyphosphate in water, it undergoes chemical reactions converting to orthophosphate making orthophosphate the most commonly identified form of phosphate in the laboratories (Fadiran *et al.*, 2008).

Although phosphate occurs naturally in the ecosystems due to the erosion of phosphate containing rocks, its natural cycle has been significantly altered, during the last 50 years, by human activities (Bennett *et al.*, 2001; Fadiran *et al.*, 2008). Since the turn of the last century, the world has witnessed an industrial and agricultural revolution, which has significantly increased the production of waste phosphates. For instance, the agricultural industry in China consumes 300, 000, 000 kg/year of pesticides to enhance the crop production (Zhang *et al.*, 2014), which in turn produces significant amounts of phosphate-contaminated drainage water. Furthermore, the global overuse of fertilisers and intensive farming practices have made agricultural effluent the major manmade source of phosphate (Wang *et al.*, 2012; Wang *et al.*, 2016). In addition, with the increasing world population, many countries continue to import huge amounts of both animal feeds and phosphate fertilisers, this long history of phosphate-containing products use have built up phosphate levels in the freshwater ecosystems of some developed countries to least 75% greater than preindustrial levels (Bennett *et al.*, 2001; Bouwman *et al.*, 2009). Beside the agricultural industry, other human activities, such as the consumption of fossil fuel, detergents, cosmetics, and other technical uses, have more than doubled the amount of wasted phosphate into the environment through the municipal and industrial wastewater (Bouwman *et al.*, 2009; Gautam *et al.*, 2014).

The excessive concentration of phosphate in water is responsible for several environmental and industrial problems (Behbahani *et al.*, 2011). For instance, the excessive presence of phosphorus, 100µg P/L, promotes the growth of alga

(eutrophication phenomenon), which in turn substantially limits sunlight penetration and the flow of carbon dioxide, subsequently depleting dissolved oxygen in the aquatic environment (Bektas *et al.*, 2004; Sibley, 2013). Industrially, the presence of phosphorus compounds in water results in costly maintenance as it promotes the fouling of water pipes (Attour *et al.*, 2014) as well as interrupting the removal of other dangerous pollutants such as arsenate (Ooi *et al.*, 2017). In addition, presence of high concentration of phosphate in drinking water results in many negative human health impacts such as loss of habitat (Bouwman *et al.*, 2009).Therefore, the Environmental Protection Agency (EPA), limits the total phosphate concentration in streams, at the point where they discharge into lakes or reservoirs, to 0.05 mg/L (WRC, 2005). In terms of drinking water limitations, the total phosphate concentration must not exceed 0.1 mg/L (Fadiran *et al.*, 2008).

To meet these limitations, a broad range of technologies have been applied to remove phosphate from water and wastewater, such as adsorption (Xu *et al.*, 2016; Ooi *et al.*, 2017), microalgae cultivation (Wang *et al.*, 2016) and reverse osmosis (Gautam *et al.*, 2014). Among this wide spectrum of phosphate removal methods, interest in electrocoagulation technology (EC) is growing as a promising alternative as it poses advantages that eliminate the drawbacks of traditional methods (Kobya *et al.*, 2010; Coman *et al.*, 2013; Hashim *et al.*, 2016; Doggaz *et al.*, 2018). For instance, the EC method, which is a process of in-situ generation of coagulants by passing an electric current through metallic electrodes, is characterised by the ease of installation and operation, short treatment time, and the ability to remove very fine particles, as these are more easily attracted to the electric field when charged (Mollah *et al.*, 2004; Dura, 2013). More importantly, EC technology does not require chemicals additives as the coagulants are freshly produced by eroding the sacrificial electrodes, which in turn prevents the generation of secondary pollutants and significantly reduces the sludge production (Kobya *et al.*, 2010; García-García *et al.*, 2015; Shaw *et al.*, 2017). Therefore, the EC method is classified as a green technology for water and wastewater treatment (Neoh *et al.*, 2016). It has been well documented that EC technology is able to remove as much as 95-99% of various pollutants within a relatively short treatment time (Gao *et al.*, 2010; Ricordel *et al.*, 2014; Hashim *et al.*, 2017b; Nariyan *et al.*, 2018). It has been successfully used to purify water of pathogens (Ricordel *et al.*, 2014), strontium (Nur *et al.*, 2017), heavy metals (Hashim *et al.*, 2017c; Martín-Domínguez *et al.*, 2018), phosphate (Behbahani *et al.*, 2011; Attour *et al.*, 2014), and organic matter (Vepsäläinen *et al.*, 2012).

However, the literature indicates that the EC method still has clear deficiencies in terms of both the lack of variety in reactor design and the availability of models for its performance. Its performance is also highly influenced by key operating parameters such as initial pH, current density (Kuokkanen, 2016; Hashim *et al.*, 2017a).

The aim of the present project is therefore to address some of these gaps in the literature. Carrying out a comprehensive study regarding optimising, assessing and the modelling of the removal of phosphates from water by the EC technology.

2. Objectives

The specific objectives of the current study are:

To investigate the feasibility of using a new aluminium (Al)-based EC reactor as a phosphate treatment method. This new reactor (PBPR) utilises perforated baffle plates as water mixers, which reduces the need for external magnetic and electrical stirrers that consumes extra power to work. The influence of electrolysis time (t) (0-60 min), initial pH value (ipH) (4 to 9), current density (J) (2 to 8 mA/cm^2), electrode spacing (ID) (5 to 15 mm) and initial phosphate concentration (IC) (50 to 150 mg/L), will be taking into considerations.

The development of an empirical model to reproduce the removal process in terms of the influence of the above operating parameters.

To conduct a preliminary estimation of the reactors' operating costs. This will provide a guide to the operating costs of the removal of phosphate from water by the Al-based EC reactor.

To calculate how much hydrogen gas (H_2) can be produced during phosphate removal, and the yieldable energy from this gas.

To carry out a SEM (scanning electron microscope) investigation of the influence of the electrocoagulation process on the morphology of the surface of aluminium electrodes.

3. Brief description of electrochemical phosphate removal

Electrocoagulation technology is an electrochemical process that depends on the in-situ generation of coagulants by passing an electric current through a sacrificial metallic anode to destabilise suspended pollutants in an aqueous media,

the cathode producing hydrogen gas that floats the pollutants (Essadki *et al.*, 2009; Vasudevan *et al.*, 2012; Heffron, 2015; Hashim *et al.*, 2017a). The type of coagulants generated depends on the material of electrodes, which is selected depending on the characteristics of the targeted pollutants, cost of material and oxidation potential (Hashim *et al.*, 2017c). Although a number of materials have been used as electrodes material in EC reactors, a wide body of literature demonstrates that aluminium is one of the most effective and successful electrode materials (Essadki *et al.*, 2009; Heffron, 2015). Because of this, aluminium (Al) has been used, in the current study, as the electrode material.

As the electric current passes through the Al electrodes, the anode starts the corrosion process producing metal cations that instantly undergo more reactions to form different polymeric metal hydroxides, similar to coagulant salts in traditional chemical coagulation processes (Essadki *et al.*, 2009; Behbahani *et al.*, 2011). These reactions at the Al electrodes and in the solution, can be summarised by the following equations (Behbahani *et al.*, 2011; Tian *et al.*, 2016; Attour *et al.*, 2015):

Anode reactions:

$$Al_{(s)} \rightarrow Al^{3+}_{(aq)} + 3e \quad \textbf{(1)}$$

$$Al^{3+}_{(aq)} + 3OH^- \rightarrow Al(OH)_3 \qquad Alkaline\ pH\ range \quad \textbf{(2)}$$

$$Al^{3+}_{(aq)} + 3H_2O \rightarrow Al(OH)_3 + 3H^+ \qquad Acidic\ pH\ range \quad \textbf{(3)}$$

Cathode reactions:

$$3H_2O + 3e \Leftrightarrow \frac{3}{2}H_2 \uparrow + 3OH^- \quad \textbf{(4)}$$

In case of phosphate present in the solution being treated, it could be precipitated according to the following reaction (Bektas *et al.*, 2004; Attour *et al.*, 2014):

$$Al^{3+}_{(aq)} + PO^{3-}_4 \rightarrow AlPO_{4(s)} \quad \textbf{(5)}$$

4. Materials and methods

4.1. Reactor construction

The electrochemical phosphates removal experiments have been carried out using a new rectangular electrocoagulation reactor (PBPR), as shown in Figure 1. This reactor consists of a Perspex rectangular container of net dimensions of length 10 cm, width of 9.5 cm and a height of 7 cm. It is supplied with six parallel-perforated rectangular baffle plates (electrodes) made from aluminium. Each electrode, width of 9.4 cm and a height of 8 cm, has 36 holes (0.4 cm in diameter) distributed in three rows and three 0.7 cm diameter holes distributed at the top and bottom to fix it in the required position. It can be seen from Figure 1(A) that the three rows of holes in the anode are shifted by 0.4 cm in comparison with those in the cathode, this is to ensure that the water follows in a convoluted path, thereby efficiently mixing the water being treated. The electrodes were held in the required position inside the reactor by 0.3 cm diameter PVC (Polyvinyl chloride) supporting rods. The distance between electrodes was controlled using

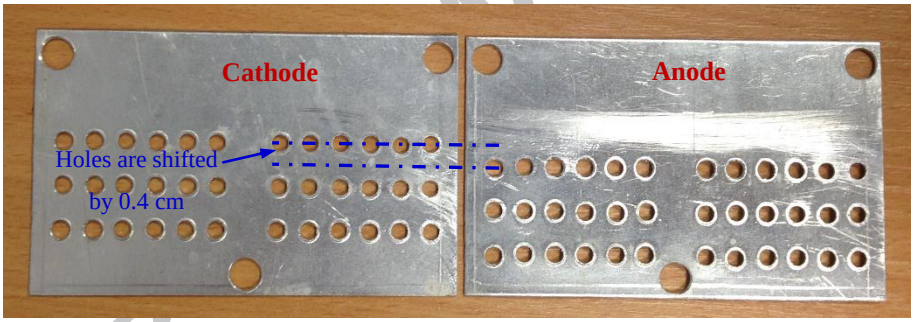

(A)

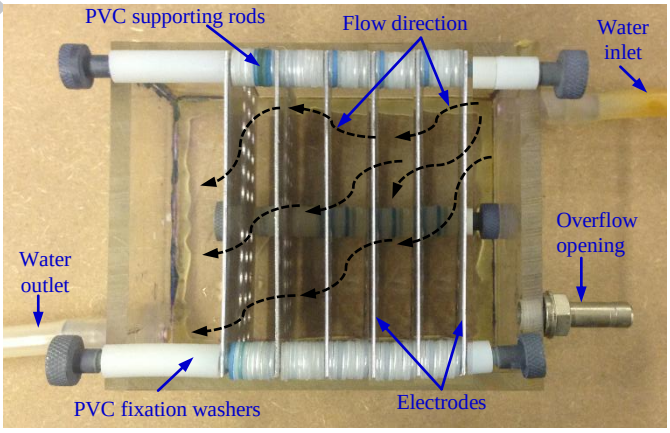

(B)

Figure 1: (A) Al electrodes, (B) The new electrocoagulation reactor (PBPR).

0.1 cm thickness PVC fixation washers. During the phosphate removal experiments, these electrodes were arranged in a monopole configuration and partially immersed in the water being treated (total effective area 304.4 cm^2).

The PBPR was connected to a peristaltic pump (Watson Marlow type, model: 504U) to circulate the water, and a rectifier (HQ Power; Model: PS 3010, 0-10 A, 0–30 V) to supply the required electrical current. Water temperature and pH values were measured using a pH/temperature pocket tester (Type: Hanna; Model: HI 98130).

4.2. Solutions

All chemicals used in the current investigation were supplied by Sigma-Aldrich and used as supplied. Water samples were collected from Al-Hila River, Iraq. The initial test of phosphate concentration in these realistic samples showed that the concentrations of phosphate were less than 20 mg/L. Thus, to check the ability of the new EC reactor to remove different concentrations of phosphate, the collected samples were spiked with phosphate up to 150 mg/L using a synthetic phosphate solution. The synthetic phosphate synthetic solution, 200 mg P/L, was prepared by dissolving 878.7 mg of potassium diphosphate (KH_2PO_4) per litre of deionised water. Samples of lower concentrations were prepared by dilution from this stock solution. The initial pH of the diluted samples was adjusted to the desired value using 1 M HCl or 1 M NaOH solutions. All the runs were carried out at room temperature (20 ± 1 ^{0}C), which was controlled using a water bath (Nickel-Electro: Clifton).

The phosphate concentration was measured using standard Hach Lange phosphate cuvettes (LCK 348-350), according to the standard method provided, and a Hach Lange spectrophotometer (Model: DR 2800).

At the end of each experiment, the electrodes were removed from the reactor, cleaned with HCl acid and rinsed with deionised water before using them in the next experiment.

4.3. Procedures and analysis

The electrochemical experiments were initiated by connecting the Al electrodes to the corresponding terminals of the rectifier. 500 mL of freshly prepared phosphate solution of the desired concentration, was fed into the PBPR and kept

circulated, using the peristaltic pump, during the course of experiment. Treatment time was started when the rectifier was switched on.

Progress of phosphate removal was monitored by collecting 0.5 mL samples from the reactor at 5-minute intervals during the course of the experiment. The collected samples were filtered with 0.45 µm filters (Sigma-Aldrich) to separate the unwanted sludge. The filtrate was then labelled and refrigerated to be tested at the end of each experiment. The residual phosphate concentration was measured, as mentioned before, using a standard phosphate cuvette test. The removal efficiency (R%) was calculated using the following equation:

$$R\% = \frac{IC-FC}{IC} \times 100\% \quad \textbf{(6)}$$

where IC and FC are the initial and final concentrations of phosphate, in mg/L, respectively.

Power consumption (C_{power}) was calculated using the following formula (Ghosh *et al.*, 2011; Un *et al.*, 2013):

$$C_{power} = \frac{I*V*t}{Vol.} \quad \textbf{(7)}$$

where C_{power} is the power consumption (W.h/m^3), I is the applied current (A), V is the potential (V), t is the electrolysis time (hrs), and *Vol.* is the volume of solution (m^3).

4.4. Modelling of phosphate removal

Several methods and techniques have been used as described in the literature, to reproduce the performance of water and wastewater treatment processes, such as the finite element method (Ulinici *et al.*, 2014), artificial neural networks (Zhang and Pan, 2014) and response surface methodology (Hakizimana *et al.*, 2017). However, the multiple regression technique (MRT), which is a family of techniques with the ability to carry out complex investigations of the interrelationships among several variables (Tabachnick and Fidell, 2001), has recently gained increasing popularity as a modelling and/or optimising statistical tool (Mustapha and Abdu, 2012; Hashim *et al.*, 2017c). Therefore, this technique has been used in the present investigation to develop an empirical model to reproduce the performance of PBPR in terms of phosphate removal. MRT encompasses standard, hierarchical and stepwise multiple regression, but the most popular is the standard multiple regression (SMR) (Pallant, 2005).

The general enhanced regression equation (Mustapha and Abdu, 2012) is:

$$Y = A + B_1X_1 + B_2X_2 + \cdots + B_kX_k + \varepsilon \quad \textbf{(8)}$$

where $Y, A, B_k, X_k,$ and ε represent the expected value of the dependant variable, the Y intercept, the regression coefficients, the independent variables and the random error coefficient (??), respectively.

The ability of the EC method to remove a pollutant from aqueous media is a function of the influence of different key operating parameters such as $t, ipH, J, ID,$ and IC (Un *et al.*, 2013; Hashim *et al.*, 2017a), which could be expressed by the following formula:

$$Removal\ of\ a\ pollutant = f(t, ipH, J, ID, \dots etc) \quad \textbf{(9)}$$

In the current investigation, the influence of $t, ipH, J, ID,$ and IC on the electrochemical phosphate removal was investigated. Therefore, in the current study, equation 9 could be written as follows:

$$R\%\ of\ phosphate = f(t, ipH, J, ID, IC) \quad \textbf{(10)}$$

In order to develop an SMR model based on the formula stated above, the following three basic steps are crucial to ensure the reliability of the model: (1) examination of the assumptions of the MRT, (2) evaluation of the developed model, and (3) assessment of the contribution of each independent variable (Pallant, 2005; Hashim *et al.*, 2017b).

4.4.1. Examination of the assumptions of the SMR

The development of an SMR model must start by checking the basic assumptions of the MRT, which are the generalisability, multicollinearity, outliers, the nature of the variables' relationships and the distribution of scores (Pallant, 2005; Hashim *et al.*, 2017c). Normally distributed data is preferred for the MRT technique.

The normality of data can be established using the Kolmogorov-Smirnov test and the z-value of skewness (Z_s) and kurtosis (Z_k). The statistical significance (ρ) of this test for normally distributed data, must be greater than 0.05, while the z-value of both Z_s and Z_k, (equations 11 and 12), must be within the range of ± 1.96 (Heffron, 2015; Musheer *et al.*, 2016; Sleight *et al.*, 2017; Shiota *et al.*, 2017).

$$Z_k = \frac{K}{S_k} \quad \textbf{(11)}$$

$$Z_s = \frac{S}{S_s} \quad \textbf{(12)}$$

where K, S_k, S and S_s are the calculated kurtosis, the standard error for kurtosis, skewness and the standard error for skewness, respectively.

The generalisability of the developed SMR model is determined by the size of the dataset, as the MRT is not applicable for small datasets (Pallant, 2005). Tabachnick and Fidell (2001) developed the following equation to calculate the minimum required number of data points to develop a generalisable SMR model:

$$Number\ of\ observations > 50 + 8m \quad \textbf{(13)}$$

where *m* is the number of independent variables.

The existence of both multicollinearity and outliers within a dataset negatively influences the outcomes of the SMR model (Tabachnick and Fidell, 2001). The existence of multicollinearity, which indicates an unwanted relationship between two independent variables, can be established by calculating the tolerance (TO) value, where small TO values (< 0.1) indicate the existence of the multicollinearity (O'Brien, 2007):

$$TO = 1 - R^2 \quad \textbf{(14)}$$

where R^2 is the coefficient of determination of a regression.

Outliers are defined as data points that are extremely different from the mean of dataset, these extreme point significantly influencing the outcomes of the developed model (Hashim *et al.*, 2017b). Therefore, outliers must be removed from the data before performing the MRT (Pallant, 2005). The presence of outliers can be established by calculating the standardised residuals (SR) for the data, any data point with an SR value out with the range 3.3 to -3.3 considered an outlier. Mahalanobis distance (MD) should be calculated for the detected outliers to check whether they need an additional analysis or not. Any outlier with an MD value greater than the critical MD could have a negative

influence on the outcome of the model (Hashim *et al.*, 2017c). The critical MD values can be calculated by equation 15, which has been developed using the critical values provided by Pallant (2005).

$$\boldsymbol{Critical\ MD\ value} = -0.0713 \times m^2 + 2.7304 \times m + 8.6739 \quad \textbf{(15)}$$

Eq. 15 is applicable to a maximum of 7 independent parameters.

Finally, the nature of the variables' relationships and the distribution of scores (i.e., the normality, linearity and homoscedasticity of residuals) can be examined by creating a scatterplot of the standardised residuals (SR), where it is expected that less than 1% of the SR values of the data will exceed the range 3.0 to -3.0 (Pallant, 2005).

4.4.2. Evaluation of the developed model.

This step of the modelling process examines the ability of the developed model to explain variations in the dependent variable (DV), the reliability of the model. Although there are many statistical tools to check reliability, the coefficient of determination (R^2) is one of the more widely used tools to achieve this goal (Field, 2008; Jafer *et al.*, 2016). The R^2 value should be between 0 and 1: the higher the R^2, the better the prediction ability.

4.4.3. Assessment of the contribution of each independent variable

The final step in the modelling process regards the influence each independent variable (IV) has on the outcome of the developed model. The contribution of each IV to the SMR model is evaluated by determining its ρ-value, the latter indicating whether each IV makes a statistically significant contribution to the model or not. Any IV with a ρ-value less than 0.05, makes an important contribution to the SMR model (Pallant, 2005). Additionally, the Beta coefficient, which is an effective statistical toll to compare the influence of the studied parameter on the outcomes of the SMR model (Hashim *et al.*, 2017b), has been calculated.

The statistical analyses in the current study was conducted using SPSS-23 package.

4.5. Economic analysis

The aim of this part of study is to explain the approach taken to estimate the operating cost of phosphate removal from water using a lab scale EC unit. The operating costs include fixed costs such as construction and equipment costs, and running costs including the cost of energy, chemicals, sludge treatment, labour and maintenance (Kobya *et al.*, 2009; Hashim *et al.*, 2017c).

However, the operating costs of a lab scale EC unit only comprise the cost of energy, chemicals, and electrode material (Kobya *et al.*, 2009; Ozyonar and Karagozoglu, 2011). In the current study therefore, the following equation has been used to calculate operating costs:

$$Operating\ cost = \alpha\ C_{power} + \gamma\ C_{material} + \beta\ C_{chemicals} \quad \textbf{(16)}$$

where C_{power} (kWh/m^3), $C_{material}$ (kg Al/m^3), and $C_{chemical}$ (kg /m^3) are the consumed power, electrode material and chemicals, respectively. α, ??, and β are the unit prices of energy, electrode material and chemicals, respectively.

The amount of electrode material consumed during the electrolysing process is calculated using Faraday's Law (Equation 17).

$$C_{material} = \frac{I \times t \times m}{Z \times F} \times 10^{-3} \quad \textbf{(17)}$$

$C_{material}$ is the lost mass of the anode (kg), I the applied current (A), t the treatment time (second), m the molecular weight of electrode material (26.98 g/mol for Al), Z the number of electrons (3 for Al) and F Faraday's constant (96487 C/mol).

4.6. Hydrogen gas production

Like any other treatment method, EC units produce some by-products such as hydrogen gas (H_2). This gas is considered one of the most useful advantages of EC technology, as it is categorised as a high energy fuel (Eker and Kargi, 2010; Lakshmi *et al.*, 2013). Therefore, the collection and conversion of the H_2 gas generated during the electrolysing process into electrical energy could minimise the energy demands of the whole process. Phalakornkule *et*

al. (2010) demonstrated that about 5.8 to13% of the energy demand of the EC cell could be obtained from conversion of H_2 gas into electrical energy.

The amount of H_2 gas produced by an EC unit can be estimated using the following formula (Phalakornkule *et al.*, 2010):

$$Q_{H_2} = \frac{J \,.\, A \,.\, t \,.\, H}{F} \quad \textbf{(18)}$$

where, Q_{H_2}, J, A, t, H, and F are the amount of H_2 gas (mole), applied current density in (A/m^2), effective surface area of electrodes (m^2), treatment time (sec), number of hydrogen molecules (1/2) and Faraday's constant (96,500), respectively.

Taking into account that each 1.0 mole of H_2 gas contains 0.244 MJ of energy, which is enough to generate 0.0678 kWh of power (Phalakornkule *et al.*, 2010; Hashim *et al.*, 2017c), the power contents (P_{H_2}) of the collected H_2 gas can be calculated using the equation:

$$P_{H_2}(\text{kWh}) = Q_{H_2} \times 0.0678 \quad \textbf{(19)}$$

4.7. Influence of the electrochemical phosphate removal on the morphology of the surface of electrodes

The SEM study has been carried out to establish the influence of the electrochemical phosphate removal process on the morphology of the surface of Al anode using an electron microscopy (FEI SEM model Inspect S) with an accelerating voltage of 25 kV.

To achieve this goal, two square pieces ($8 \times 8\ mm$) of the Al anode, before and after the electrocoagulation process, were cleaned and dried, and then characterised by the scanning electron microscopy.

5. Results and discussion

5.1. Experimental work

5.1.1. Influence of initial pH

It has been widely reported that the EC process is highly sensitive to the pH value as the latter governs the speciation of Al hydroxides which in turn influence removal efficiency (Attour *et al.*, 2014; García-García *et al.*, 2015).

Therefore, the influence of this key parameter on phosphate removal has been investigated by treating 100 mg/L phosphate containing solutions of different initial pH values (4 to 9) for 60 minutes. The J and ID were kept constant at 4 mA/cm^2 and 0.5 cm, respectively. Figure 2-(A) illustrates phosphate removal efficiency for different initial pH values. It can be clearly seen that a slightly acidic environment is preferable for the electrochemical removal of

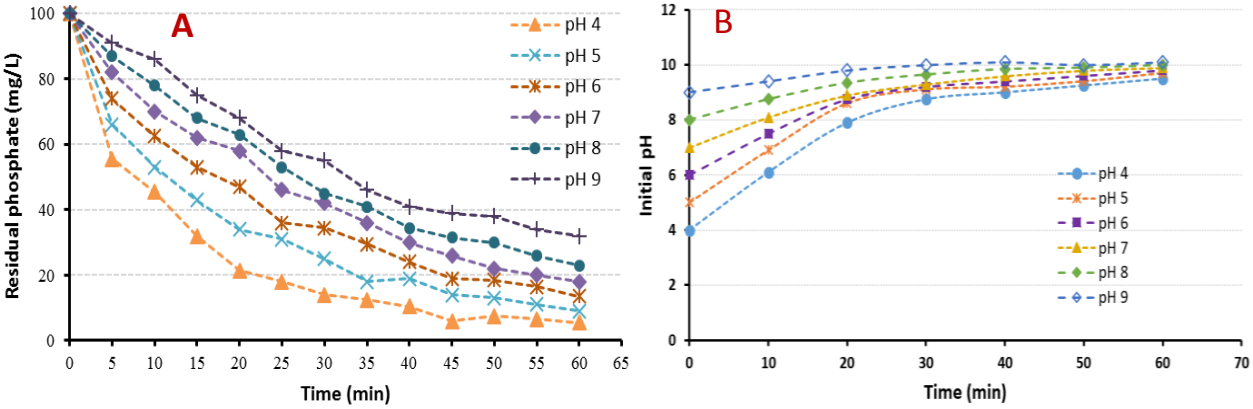

Figure 2: A) Phosphate removal efficiency versus treatment time for different initial pH values, B) pH level versus treatment time.

phosphate from water.

This can be explained by columbic attraction, where in the acidic range of the pH, the surface of freshly produced coagulants exhibits a positive charge, which enhances the removal of anionic phosphate. In basic pH ranges, coagulants exhibit a negative charge that repulses anionic phosphate, this decreasing removal efficiency (Kobya *et al.*, 2010; Behbahani *et al.*, 2011). These results are in good agreement with those of Behbahani *et al.* (2011) and Attour *et al.* (2014).

It is noteworthy to highlight that it has been noticed that the pH value increased gradually with the treatment time, Figure 2-(B). This increase in the pH value could be mainly attributed to the continuous production of OH^- at the cathode.

Following this, the remaining experiments in the current study will be carried out at an initial pH of 6, the average pH of wastewater, surface and drinking water ranging between 5 and 8.2 (Liang *et al.*, 2009; Zhu *et al.*, 2013; Zeng, 2014; Zhao *et al.*, 2017). The results also showed a minimal and non-significant decrease in phosphate removal efficiency as the initial pH increased from 4 to 6 (less than 8%).

5.1.2. Influence of current density

Current density (J) is one of the most effective operating parameters in any electrocoagulation process as it governs the anodic dissolution rate, floc's growth and rate of bubble-generation (Un *et al.*, 2009; Gao *et al.*, 2010). To study its influence on phosphate removal efficiency, four different current densities (2, 4, 6, and 8 mA/cm^2) were applied, for 60 minutes, to 100 mg/L phosphate containing samples at ID of 0.5 cm, ipH of 6, and IC of 100 mg/L.

The results obtained confirmed that the phosphate removal efficiency increased with the increase of J. It can be seen from Figure 3-(A) that PBPR required only 14 min at J 8 mA/cm^2 to remove 80 mg/L of phosphate; it took 45 min to remove the same amount of phosphate at J of 4 mA/cm^2. This could be explained by the fact that the dissolved aluminium ions from the anode increase as the J increases, and enhances flocs formation and fluoride removal as a consequence (Zhu *et al.*, 2007; Behbahani *et al.*, 2011).

However, it was observed that power consumption increased as J increased. Figure 3(B) shows an increase in power consumption from approximately 0.6 to 5.9 kW.h/m^3 as the J increased from 2 to 8 mA/cm^2, respectively. It may therefore be reasonable to infer that a J of 6 mA/cm^2 is the best value to carry out the remaining experiments.

5.1.3. Influence of the inter-electrode distance

A wide body of literature indicates that the efficiency of EC units is influenced by the distance between electrodes (ID). The latter determines the ohmic resistance of the cell, which in turn determines the production of coagulants and energy consumption (Mohora *et al.*, 2012; Shaw *et al.*, 2017). Therefore, a set of experiments was carried out to assess

its influence on phosphate removal by treating 100 mg/L phosphate solution at three different IDs (0.5, 1 and 1.5 cm), an ipH of 6, and J of 6 mA/cm^2.

The results obtained (Figure 4(A)), revealed a reverse proportional relationship between phosphate removal efficiency and ID. After 30 min of treatment, the residual concentration of phosphate increased from 14 mg/L to 32 mg/L as the ID increased from 0.5 to 1.5 cm. This is because when ID increases, coagulant production decreases, consequently decreasing removal efficiency.

Increasing ID dramatically increases energy consumption; Figure 4(B) shows that an increase in ID from 0.5 to 1.5 cm increased power consumption from 3.42 to 9.11 kWh/m^3. This increase in power consumption is due to the increase in ohmic resistance; if the ID increases, cell resistance will also increase, which in turn increases power consumption.

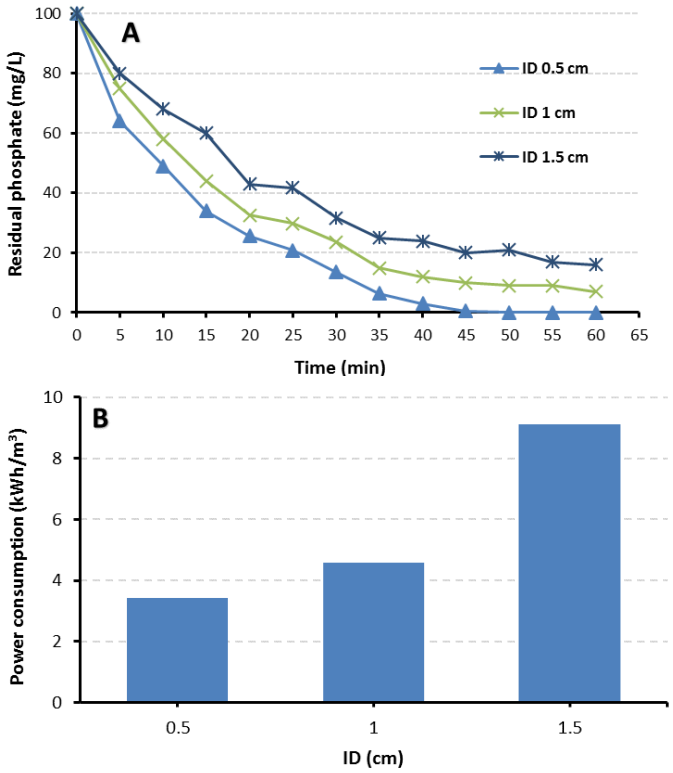

Figure 3: Influence of ID on: (A) Phosphate removal, (B) Power consumption.

Therefore, the ID was maintained at 0.5 cm for the remainder of the current investigation.

5.1.4. Influence of initial phosphate concentration

Sets of water samples with three different concentrations of phosphate (50, 100, and 150 mg/L) were treated for 60 min with an ipH of 6, ID of 0.5 cm, and J of 6 mA/cm^2, to examine the influence of the initial phosphate concertation on the performance of the PBPR.

Figure 5 shows that removal efficiency is inversely proportional to the initial concentration of phosphate, where the removal efficiency, after 30 min of treatment, decreased from 87% to 65% as the initial phosphate concentration decreased from 100 to 150 mg/L, respectively. This could be because of the availability of adsorption sites, where a constant quantity of coagulants is dissolved from the Al anode for the same J and electrolysis time, i.e., the same quantity of coagulants was produced in the PBPR during the removal of the different phosphate concentrations. The flocs generated at higher concentrations, were not sufficient to absorb all the phosphate ions. Therefore, PBPR

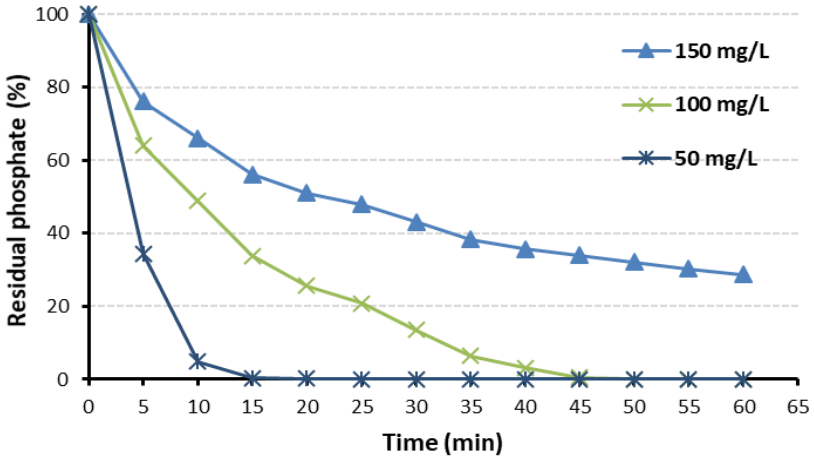

Figure 4: Phosphate removal efficiency versus treatment time for different concentrations of phosphate.

requires more time to remove high phosphate concentrations.

In summary, the obtained results confirms that about 50 min of electrolysing using the PBPR, at the optimum operating conditions, is enough to achieve a complete removal of phosphorus (0 mg/L) even when the initial concentration of phosphate is 100 mg/L.

5.2. Modelling of phosphate removal

SSPS-23 has been used, in the current study, as a statistical tool to model the variation of phosphate removal (DV) with the change in the operating parameters (IVs).

5.2.1. Examination of the assumptions of the SMR.

Initially, the normality of the collected data was examined using Kolmogorov-Smirnov test, Z_s and Z_k. The initial analysis indicated that the data was not normally distributed as the values of ρ for Kolmogorov-Smirnov, Z_s and Z_k were 0.01, 2.89, and -1.97, respectively. Therefore, before checking MRT assumptions, the dataset was screened to remove extreme outliers and then normalised (using the SQRT method) to ensure reliability of the developed model and to avoid statistical bias. The values of ρ of Kolmogorov-Smirnov, Z_s and Z_k after the normalisation process were 0.2, 0.19, and -1.91, respectively, which confirms the normality of the data. Figure 6 shows the normality plots and the Q-Q plots of the data before and after normalisation.

In terms of generalisability, the minimum number of data points required to develop a generalisable SMR model, according to Eq. 13, is 90 points. This assumption has been met as the data consists of 208 experimental readings.

The results obtained from the statistical analysis (Table 1), indicate the absence of multicollinearity within the normalised data as the TO value of each IV is greater than 0.1.

According to the calculated SR values (Table 1), there are two outliers in the data. The MD values of these points were calculated and compared to the critical MD value (Eq. 15). The results (Table 1), confirm that the MD values of these outliers were less than the critical MD value, which means they will not exert a significant influence on the outcomes of the developed model.

Finally, the results confirm that the assumptions of normality, linearity and homoscedasticity of residuals was not violated as less than 1% of the SR values lay outside the range 3.0 to -3.0.

According to the calculated coefficients (Table 1), the SMR model for phosphate removal could be written as follows:

$$R\% = (3.87 - 0.144 \times t + 0.557 \times ipH - 0.887 \times J + 2.097 \times ID + 0.045 \times IC)^2 \quad \textbf{(20)}$$

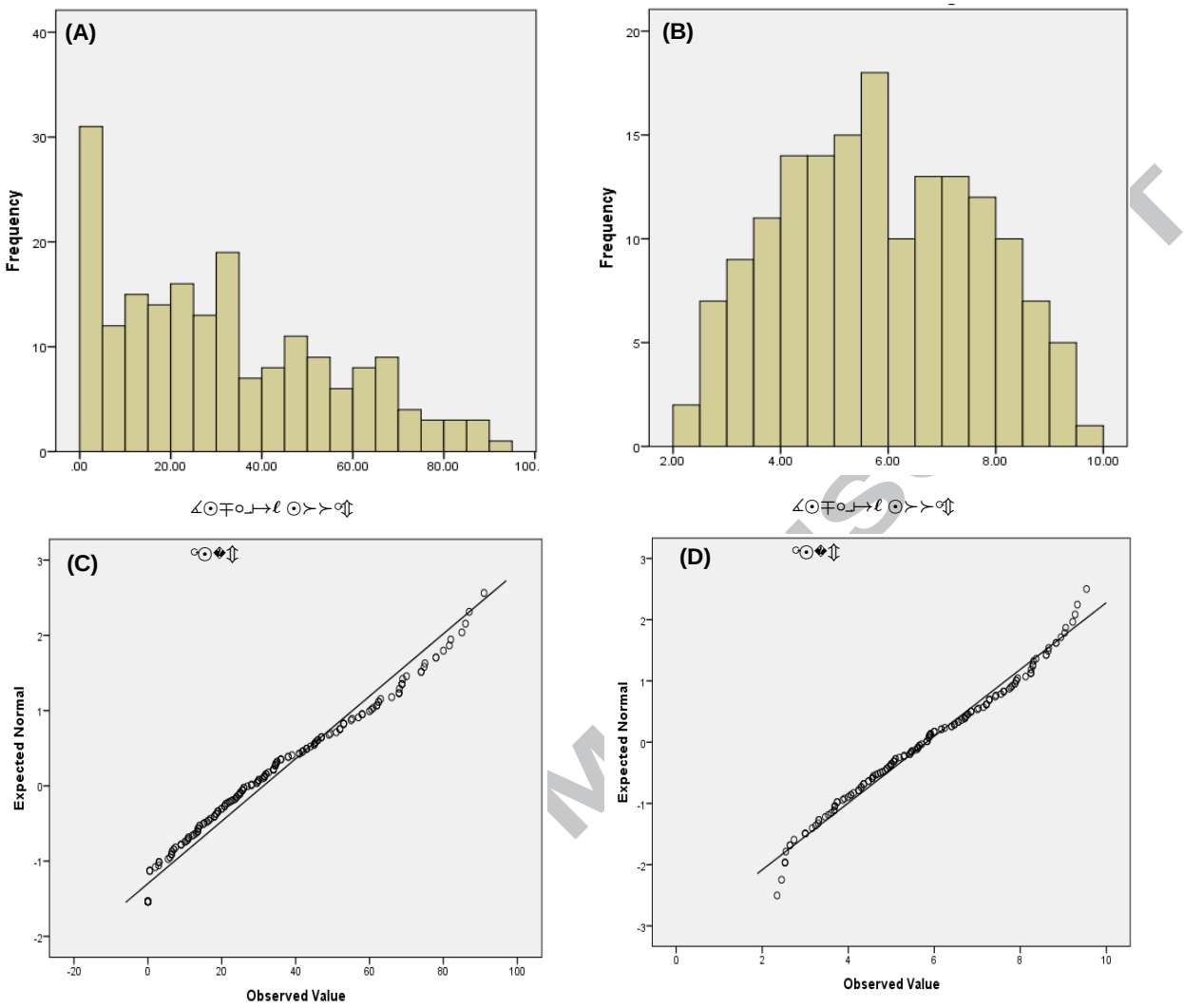

Figure 5: (A) Normality histogram of non-normalised data. (B) Normality histogram of non-normalised data (C) Q-Q plot of non-normalised data. (D) Q-Q plot of normalised data,

Table 1: Summary of the statistical analysis.

Parameters	Model coefficients	TO	Sig.	Beta	SR exceeded the range of 3.3 to -3.3		MD	SR exceeded the range of 3.0 to -3.0	
					No. of cases	SR values		No. of cases	SR values
Constant	3.870								
t	-0.144	1.00	0.00	-0.74					
ipH	0.557	0.98	0.00	0.21	118	4.123	7.883	118	4.123
J	-0.887	0.92	0.00	-0.43	170	4.688	11.332	170	4.688
ID	2.097	0.93	0.00	0.19					
IC	0.045	1.00	0.00	0.27					

5.2.2. Evaluation of the developed model.

The ability of the developed SMR model (Eq. 20), to explain variations in phosphate removal has been checked by calculating the coefficient of determination (R^2). An R^2 of 0.882 confirms the ability of the SMR model to explain 88.2% of the variance in phosphate removal performance of PBPR, which is an acceptable value for experimental data (Jafer *et al.*, 2016; Hashim *et al.*, 2017a).

5.2.3. Assessment of the contribution of each independent variable

The statistical significance (ρ-value) of each operating parameter has been calculated to check whether it influences the outcomes of the SMR model. Table 1 shows that the ρ-value of each individual operating parameter was less than 0.05, indicating that all the parameters contribute to the outcome of the model. However, each operating parameter exerts a different influence that varies from ignorable to significant. The Beta coefficient, which measures how strongly each parameter influences the outcomes of the SMR model, has been calculated for each parameter. Figure 7

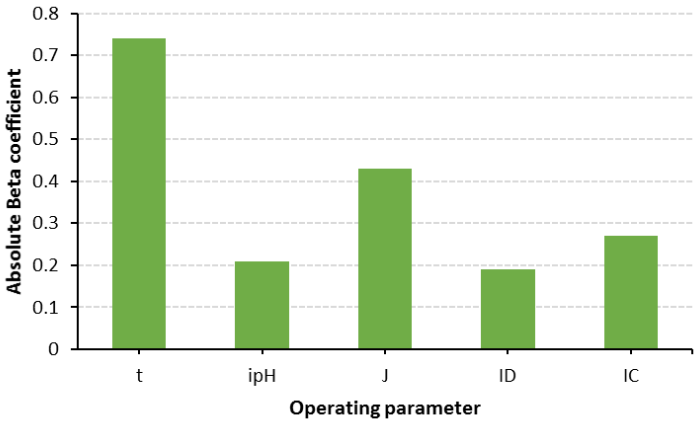

Figure 6: Absolute Beta coefficients of the operating parameters.

illustrates that influence following the order: $t >$ J $>$ IC $>$ ipH $>$ ID.

Finally, the SMR model was applied to a randomly selected dataset, 50 points of experimental data. This random dataset was selected using SPSS-23 software to avoid any statistical bias. Figure 8 shows very good agreement between measured and predicted phosphate removal efficiencies, the R^2 value for this random sample 0.869.

In conclusion, based on the results of the statistical analysis, the developed SMT model could be used to reproduce the performance of the PBPR in terms of phosphate removal from water. However, this model is only applicable within the range of operating parameters included here; a wider / different range could result in different outcomes. Further

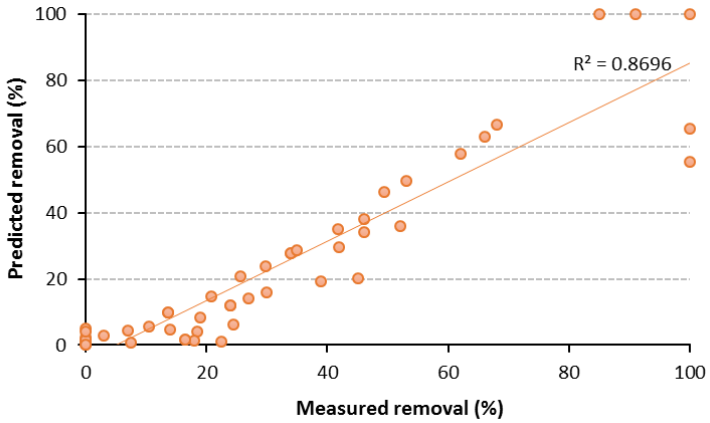

Figure 7: Measured versus predicted phosphate removal for randomly selected data points.

research with wider ranges of operating parameters should be carried out to develop more generalisable model.

5.3. Economic analysis

In the current preliminary economic study, the operating cost for phosphate removal from water using PBPR was calculated according to the unit prices of the Iraqi market in August 2017 (14 pence/kWh of electricity, and 1.53$/kg of Al).

The amount of energy consumed and electrode material used were calculated according to equations 7 and 17, respectively, the amount of chemicals calculated experimentally. The minimum operating cost for phosphate removal, according to Eq. 16, in this study is:

$$Operating\ cost = \frac{14}{100} \times 3.42 + 1.53 \times 0.574 \times 10^{-3} + 0.023 = 0.503\ \frac{US\ \$}{m^3}$$

This cost is comparable with that documented for EC methods in the literature. Ozyonar and Karagozoglu (2011) reported that the cost to remove COD, turbidity and phosphorus using an EC cell at a current density of 1-15 mA/cm^2

as approximately 0.86 \$/m^3. Hashim *et al.* (2017b) reported the minimum required cost for electrochemical nitrate removal from drinking water to be 0.455 \$/m^3.

It is noteworthy to mention that, according to the literature, the iron-based electrocoagulation is cheaper than aluminium-based electrocoagulation (Lacasa *et al.*, 2013). However, the aluminium electrodes are more efficient than the iron electrodes in terms anion removal, they produce larger flocs in comparison with iron electrodes, and aluminium is much lighter than iron that greatly facilitates the installation and mobility of the electrocoagulation units (Behbahani *et al.*, 2011; Hashim *et al.*, 2017b; Vainio, 2017).

5.4. Hydrogen gas production

Quantification of H_2 gas emissions from the FCER during electrochemical phosphate removal, was carried out using Eq. 21 as follows:

$$Q_{H_2} = \frac{60 * 0.0285 * 3600 * 0.5}{96500} = 0.032 \text{ mole}$$

This amount of H_2 gas is produced during the treatment of 0.5 L of phosphate solution, equivalent to 64 mole/m^3. The amount of electrical power produced by recycling the H_2 gas emitted during the electrochemical phosphate removal from water, according to Eq. 19, is:

$$P_{H_2} = 64 \times 0.0678 = 4.34 \frac{kWh}{m^3}$$

These results show that a considerable amount of energy could be obtained by recycling H_2 gas emitted from field-scale EC plants.

5.5. Influence of the electrochemical phosphate removal on the morphology of the surface of electrodes

SEM technology was used to examine the influence of the electrochemical phosphate removal process on the morphology of the Al anode surface. The SEM images of the Al anode, before and after the treatment process, are shown in Figure 8. It can clearly be seen from the images that the initially smooth surface of the Al anode became

rough and nonuniform after several electrolysing runs, this related to the passivation of the Al anode due to the product ion of coagulants.

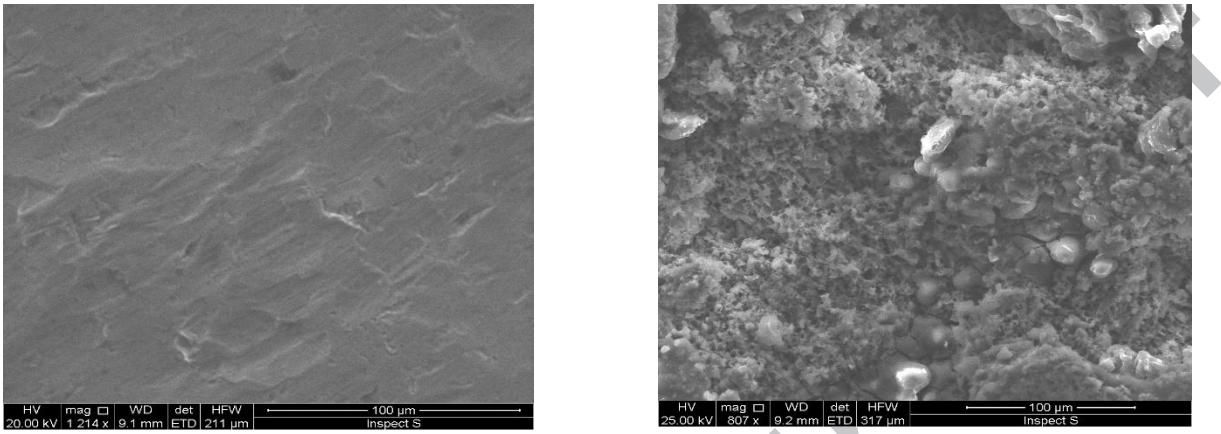

(A) **(B)**

Figure 8: SEM images of Al anode, (A) before the EC process, and (B) after the EC process.

6. Conclusion

The current study investigated the suitability of using a new Al-based electrocoagulation unit for the treatment of water with high concentrates of phosphate. This study also investigated the applicability of the multiple regression technique to model phosphate removal performance taking into consideration the influence of key operating parameters. The results obtained indicate that phosphate removal is more efficient at slightly acidic pH levels, the phosphate removal proportional to a combination of both current density and electrolysis period. In contrast, phosphate removal is inversely proportional to the distance between electrodes and the initial concentration of phosphate. Statistically, it has been illustrated that the influence of the key operating parameters on the phosphate removal performance of the electrocoagulation unit could be modelled with R^2 of 0.882.

Additionally, perhaps most importantly, the outcomes of this study indicated that the new bench scale baffle plates reactor (FCER) achieved similar phosphate removal efficiency to those in literature without the need for external mechanical or magnetic stirrers which require extra power to work. Therefore, FCER could be a cost-effective alternative to the traditional lab-scale EC reactors. Furthermore, the electrocoagulation method could be used for

economic phosphate removal due to the potential to produce a considerable amount of energy by recycling emitted H_2 gas.

For future work, the empirical model developed here could be enhanced by including the influence of other operating parameters (such as water temperature) and/or by studying wider ranges of the parameters already included. The sludge which is produced could be characterised using SEM technology, this providing information regarding the development of better sludge handling methods.

Acknowledgement

This work is supported by the University of Babylon and Liverpool John Moores University (LJMU). The authors are very grateful to the technicians from LJMU who provided the expertise needed to assist with this investigation.

References

Attour, A., Ben Grich, N., Mouldi Tlili, M., Ben Amor, M., Lapicque, F.and Leclerc, J.-P. 2015. Intensification of phosphate removal using electrocoagulation treatment by continuous pH adjustment and optimal electrode connection mode. *Desalination and Water Treatment***,** 1-8.

Attour, A., Touati, M., Tlili, M., Ben Amor, M., Lapicque, F.and Leclerc, J. P. 2014. Influence of operating parameters on phosphate removal from water by electrocoagulation using aluminum electrodes. *Separation and Purification Technology,* 123**,** 124-129.

Barca, C., Gerente, C., Meyer, D., Chazarenc, F.and Andres, Y. 2012. Phosphate removal from synthetic and real wastewater using steel slags produced in Europe. *Water Res,* 46.

Behbahani, M., Moghaddam, M. R. A.and Arami, M. 2011. A Comparison Between Aluminum and Iron Electrodes on Removal of Phosphate from Aqueous Solutions by Electrocoagulation Process. *Int. J. Environ. Res.,* 5**,** 403-412.

Bektas, N., Akbulut, H., Inan, H.and Dimoglo, A. 2004. Removal of phosphate from aqueous solutions by electro-coagulation. *J Hazard Mater,* 106**,** 101-5.

Bennett, E. M., Carpenter, S. R.and Caraco, N. F. 2001. Human Impact on Erodable Phosphorus and Eutrophication: A Global Perspective: Increasing accumulation of phosphorus in soil threatens rivers, lakes, and coastal oceans with eutrophication. *AIBS Bulletin,* 51**,** 227-234.

Bouwman, A. F., Beusen, A. H. W.and Billen, G. 2009. Human alteration of the global nitrogen and phosphorus soil balances for the period 1970-2050. *Global Biogeochemical Cycles,* 23**,** n/a-n/a.

Coman, V., Robotin, B.and Ilea, P. 2013. Nickel recovery/removal from industrial wastes: a review. *Resources, Conservation and Recycling,* 73**,** 229-238.

Doggaz, A., Attour, A., Le Page Mostefa, M., Tlili, M.and Lapicque, F. 2018. Iron removal from waters by electrocoagulation: Investigations of the various physicochemical phenomena involved. *Separation and Purification Technology*.

Dura, A. 2013. *Electrocoagulation for Water Treatment: the Removal of Pollutants using Aluminium Alloys, Stainless Steels and Iron Anodes.* PhD thesis, National University of Ireland Maynooth.

Eker, S.and Kargi, F. 2010. Hydrogen gas production from electrohydrolysis of industrial wastewater organics by using photovoltaic cells (PVC). *International Journal of Hydrogen Energy,* 35**,** 12761-12766.

Essadki, A. H., Gourich, B., Vial, C., Delmas, H.and Bennajah, M. 2009. Defluoridation of drinking water by electrocoagulation/electroflotation in a stirred tank reactor with a comparative performance to an external-loop airlift reactor. *J Hazard Mater,* 168**,** 1325-33.

Fadiran, A. O., Dlamini, S. C.and Mavuso, A. 2008. A comparative study of the phosphate levels in some surface and ground water bodies of Swaziland. *Bull. Chem. Soc. Ethiop.*, 22**,** 197-206.

Field, A. 2008. *Multiple regression using SPSS. Research Methods in Psychology,* C8057, pp.1-11.

Gao, S., Yang, J., Tian, J., Ma, F., Tu, G.and Du, M. 2010. Electro-coagulation-flotation process for algae removal. *J Hazard Mater,* 177**,** 336-43.

García-García, A., Martínez-Miranda, V., Martínez-Cienfuegos, I. G., Almazán-Sánchez, P. T., Castañeda-Juárez, M.and Linares-Hernández, I. 2015. Industrial wastewater treatment by electrocoagulation–electrooxidation processes powered by solar cells. *Fuel,* 149**,** 46-54.

Gautam, R. K., Banerjee, S., Gautam, P. K.and Chattopadhyaya, M. 2014. Remediation Technologies for Phosphate Removal From Wastewater: An Overview. *Adv. Environ. Res.*, 36**,** 177-200.

Ghosh, D., Medhi, C. R.and Purkait, M. K. 2011. Techno-economic analysis for the electrocoagulation of fluoride-contaminated drinking water. *Toxicological & Environmental Chemistry,* 93**,** 424-437.

Hakizimana, J. N., Gourich, B., Chafi, M., Stiriba, Y., Vial, C., Drogui, P.and Naja, J. 2017. Electrocoagulation process in water treatment: A review of electrocoagulation modeling approaches. *Desalination,* 404**,** 1-21.

Hashim, K. S., Shaw, A., Al Khaddar, R., Ortoneda Pedrola, M.and Phipps, D. 2017a. Defluoridation of drinking water using a new flow column-electrocoagulation reactor (FCER) - Experimental, statistical, and economic approach. *J Environ Manage,* 197**,** 80-88.

Hashim, K. S., Shaw, A., Al Khaddar, R., Pedrola, M. O.and Phipps, D. 2017b. Energy efficient electrocoagulation using a new flow column reactor to remove nitrate from drinking water - Experimental, statistical, and economic approach. *J Environ Manage,* 196**,** 224-233.

Hashim, K. S., Shaw, A., Al Khaddar, R., Pedrola, M. O.and Phipps, D. 2017c. Iron removal, energy consumption and operating cost of electrocoagulation of drinking water using a new flow column reactor. *Journal of Environmental Management,* 189**,** 98-108.

Hashim, K. S., Shaw, A., Alkhaddar, R., Pedrola, M. O.and Phipps, D., 2016. Effect of the supporting electrolyte concentration on energy consumption and defluoridation of drinking water in the electrocoagulation (EC) method. *The 2nd BUiD Doctoral Research Conference*. The British University in Dubai.

Heffron, J. 2015. *Removal of Trace Heavy Metals from Drinking Water by Electrocoagulation.* MSc thesis, Marquette University.

Jafer, H. M., Hashim, K. S., Atherton, W.and Alattabi, A. W. 2016. A Statistical Model for the Geotechnical Parameters of Cement-Stabilised Hightown's Soft Soil: A Case Stufy of Liverpool, UK. *World Academy of Science, Engineering and Technology, International Journal of Civil, Environmental, Structural, Construction and Architectural Engineering,* 10**,** 931-936.

Kobya, M., Demirbas, E.and Akyol, A. 2009. Electrochemical treatment and operating cost analysis of textile wastewater using sacrificial iron electrodes. *Water Sci Technol,* 60**,** 2261-70.

Kobya, M., Demirbas, E., Dedeli, A.and Sensoy, M. T. 2010. Treatment of rinse water from zinc phosphate coating by batch and continuous electrocoagulation processes. *J Hazard Mater,* 173**,** 326-34.

Kuokkanen, V. 2016. *Utilization of electrocoagulation for water and wastewater treatment and nutrient recovery. Techno-economic studies.* PhD thesis, University of Oulu Graduate School; University of Oulu.

Lacasa, E., Cañizares, P., Sáez, C., Fernández, F. J.and Rodrigo, M. A. 2011. Electrochemical phosphates removal using iron and aluminium electrodes. *Chemical Engineering Journal,* 172**,** 137-143.

Lacasa, E., Cañizares, P., Sáez, C., Martínez, F.and Rodrigo, M. A. 2013. Modelling and cost evaluation of electro-coagulation processes for the removal of anions from water. *Separation and Purification Technology,* 107**,** 219-227.

Lakshmi, J., Sozhan, G.and Vasudevan, S. 2013. Recovery of hydrogen and removal of nitrate from water by electrocoagulation process. *Environ Sci Pollut Res,* 20**,** 2184–2192.

Liang, S., Guo, X., Feng, N.and Tian, Q. 2009. Application of orange peel xanthate for the adsorption of Pb2+ from aqueous solutions. *J Hazard Mater,* 170**,** 425-9.

Martín-Domínguez, A., Rivera-Huerta, M. L., Pérez-Castrejón, S., Garrido-Hoyos, S. E., Villegas-Mendoza, I. E., Gelover-Santiago, S. L., Drogui, P.and Buelna, G. 2018. Chromium removal from drinking water by redox-assisted coagulation: Chemical versus electrocoagulation. *Separation and Purification Technology,* 200**,** 266-272.

Mohora, E., Roncevic, S., Dalmacija, B., Agbaba, J., Watson, M., Karlovic, E.and Dalmacija, M. 2012. Removal of natural organic matter and arsenic from water by electrocoagulation/flotation continuous flow reactor. *J Hazard Mater,* 235-236**,** 257-64.

Mollah, M. Y., Morkovsky, P., Gomes, J. A., Kesmez, M., Parga, J.and Cocke, D. L. 2004. Fundamentals, present and future perspectives of electrocoagulation. *J Hazard Mater,* 114**,** 199-210.

Musheer, Z., Govil, P.and Gupta, S. 2016. Attitude of Secondary Level Students towards Their School Climate. *Journal of Education and Practice,* 7**,** 39-45.

Mustapha, A.and Abdu, A. 2012. Application of Principal Component Analysis & Multiple Regression Models in Surface Water Quality Assessment. *Journal of Environment and Earth Science,* 2**,** 16-23.

Nariyan, E., Sillanpää, M.and Wolkersdorfer, C. 2018. Uranium removal from Pyhäsalmi/Finland mine water by batch electrocoagulation and optimization with the response surface methodology. *Separation and Purification Technology,* 193**,** 386-397.

Neoh, C. H., Noor, Z. Z., Mutamim, N. S. A.and Lim, C. K. 2016. Green technology in wastewater treatment technologies: Integration of membrane bioreactor with various wastewater treatment systems. *Chemical Engineering Journal,* 283**,** 582-594.

Nur, T., Loganathan, P., Kandasamy, J.and Vigneswaran, S. 2017. Removal of strontium from aqueous solutions and synthetic seawater using resorcinol formaldehyde polycondensate resin. *Desalination,* 420**,** 283-291.

O'brien, R. M. 2007. A Caution Regarding Rules of Thumb for Variance Inflation Factors. *Quality & Quantity,* 41**,** 673-690.

Ooi, K., Sonoda, A., Makita, Y.and Torimura, M. 2017. Comparative study on phosphate adsorption by inorganic and organic adsorbents from a diluted solution. *Journal of Environmental Chemical Engineering,* 5**,** 3181-3189.

Ozyonar, F.and Karagozoglu, B. 2011. Operating Cost Analysis and Treatment of Domestic Wastewater by Electrocoagulation Using Aluminum Electrodes. *Polish J. of Environ. Stud,* 20**,** 173-179.

Pallant, J. 2005. *SPSS SURVIVAL MANUAL,* Australia, Allen & Unwin.

Phalakornkule, C., Sukkasem, P.and Mutchimsattha, C. 2010. Hydrogen recovery from the electrocoagulation treatment of dye-containing wastewater. *International Journal of Hydrogen Energy,* 35**,** 10934-10943.

Ricordel, C., Miramon, C., Hadjiev, D.and Darchen, A. 2014. Investigations of the mechanism and efficiency of bacteria abatement during electrocoagulation using aluminum electrode. *Desalination and Water Treatment,* 52**,** 5380-5389.

Shaw, A., Hashim, K. S., Alkhaddar, R., Pedrola, M. O.and Phipps, D., 2017. Influence of electrodes spacing on internal temperature of electrocoagulation (EC) cells during the removal (Fe II) from drinking water. *The 3rd BUiD Annual Doctoral Research Conference*. The British University, Dubai.

Shiota, S., Okamoto, Y., Okada, G., Takagaki, K., Takamura, M., Mori, A., Yokoyama, S., Nishiyama, Y., Jinnin, R., Hashimoto, R. I.and Yamawaki, S. 2017. Effects of behavioural activation on the neural basis of other perspective self-referential processing in subthreshold depression: a functional magnetic resonance imaging study. *Psychol Med,* 47**,** 877-888.

Sibley, B. 2013. *Phosphorus Control in Passive Wastewater Treatment and Retention Works Using Water Treatment Residual Solids.* Master thesis, University of Saskatchewan.

Sleight, V. A., Bakir, A., Thompson, R. C.and Henry, T. B. 2017. Assessment of microplastic-sorbed contaminant bioavailability through analysis of biomarker gene expression in larval zebrafish. *Mar Pollut Bull,* 116**,** 291-297.

Strileski, M. 2013. *Phosphorus removal from EBPR sludge dewatering liquors using lanthanum chloride, aluminum sulfate and ferric chloride.* PhD thesis, University of Nevada, Las Vegas.

Tabachnick, B. G.and Fidell, L. S. 2001. *Using Multivariate Statistics,* Boston, Allyn and Bacon.

Tian, Y., He, W., Zhu, X., Yang, W., Ren, N.and Logan, B. E. 2016. Energy efficient electrocoagulation using an air-breathing cathode to remove nutrients from wastewater. *Chemical Engineering Journal,* 292**,** 308-314.

Ulinici, S. C., Vlad, G., Vâju, D., Balint, I., Băisan, G.and Hetvary, M. 2014. Numerical modeling of processes in water treatment plants as a basis for an optimal design. *Journal of Environmental Research and Protection,* 11**,** 41- 57.

Un, U. T., Koparal, A. S.and Bakir Ogutveren, U. 2009. Electrocoagulation of vegetable oil refinery wastewater using aluminum electrodes. *J Environ Manage,* 90**,** 428-33.

Un, U. T., Koparal, A. S.and Bakir Ogutveren, U. 2013. Fluoride removal from water and wastewater with a bach cylindrical electrode using electrocoagulation. *Chemical Engineering Journal,* 223**,** 110-115.

Vainio, H. 2017. *Suitability of electrocoagulation and filtration for mining water treatment.* MSc Lappeenranta University of Technology.

Vasudevan, S., Lakshmi, J.and Sozhan, G. 2012. Simultaneous removal of Co, Cu, and Cr from water by electrocoagulation. *Toxicological & Environmental Chemistry,* 94**,** 1930-1940.

Vepsäläinen, M., Pulliainen, M.and Sillanpää, M. 2012. Effect of electrochemical cell structure on natural organic matter (NOM) removal from surface water through electrocoagulation (EC). *Separation and Purification Technology,* 99**,** 20-27.

Wang, P., Tian, Y., Wang, X. J., Gao, Y., Shi, R., Wang, G. Q., Hu, G. H.and Shen, X. M. 2012. Organophosphate pesticide exposure and perinatal outcomes in Shanghai, China. *Environ Int,* 42**,** 100-4.

Wang, X. X., Wu, Y. H., Zhang, T. Y., Xu, X. Q., Dao, G. H.and Hu, H. Y. 2016. Simultaneous nitrogen, phosphorous, and hardness removal from reverse osmosis concentrate by microalgae cultivation. *Water Res,* 94**,** 215-24.

Water Research Center (WRC), 2005. Phosphates in the Environment /Phosphorus and water quality. *Phosphates in the Environment /Phosphorus and water quality.* Geoenvironmental Sciences and Engineering Department. http://www.water-research.net/index.php/phosphates.

Xu, H., Zhu, B., Ren, X., Shao, D., Tan, X.and Chen, C. 2016. Controlled synthesized natroalunite microtubes applied for cadmium(II) and phosphate co-removal. *J Hazard Mater,* 314**,** 249-59.

Zeng, C. 2014. *Application of UV LEDs for Turbid Wastewater Disinfection.* Master thesis, Asian Institute of Technology.

Zhang, Y., Han, S., Liang, D., Shi, X., Wang, F., Liu, W., Zhang, L., Chen, L., Gu, Y.and Tian, Y. 2014. Prenatal exposure to organophosphate pesticides and neurobehavioral development of neonates: a birth cohort study in Shenyang, China. *PLoS One,* 9**,** e88491.

Zhang, Y.and Pan, B. 2014. Modeling batch and column phosphate removal by hydrated ferric oxide-based nanocomposite using response surface methodology and artificial neural network. *Chemical Engineering Journal,* 249**,** 111-120.

Zhao, R. J., Gong, L. Y., Zhu, H. D., Liu, Q., Xu, L. X., Lu, L.and Yang, Q. Z. 2017. Property of filler-loaded magnetic ferrite from plastic waste bottle used to treat municipal domestic sewage. *Environ Technol***,** 1-7.

Zhu, J., Zhao, H.and Ni, J. 2007. Fluoride distribution in electrocoagulation defluoridation process. *Separation and Purification Technology,* 56**,** 184-191.

Zhu, X., Chen, Y., Chen, H., Li, X., Peng, Y.and Wang, S. 2013. Minimizing nitrous oxide in biological nutrient removal from municipal wastewater by controlling copper ion concentrations. *Appl Microbiol Biotechnol,* 97**,** 1325-34.

Graphical abstract

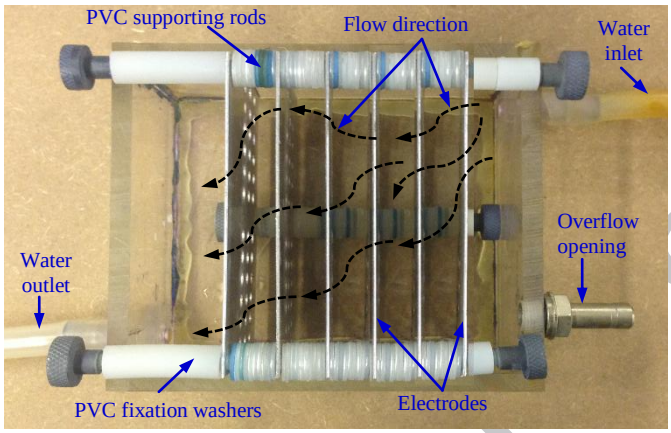

Highlights

- The new aluminium-based EC reactor, PBPR, removed 99 mg/L of phosphate within 60 minutes.
- PBPR produced enough hydrogen gas to generate 4.34 kWh/m^3 of power.
- The influence of the operating parameters on phosphate removal could be modelled with an R^2 of 0.882
- SEM images showed many dents on the anode due to the production of Al hydroxides.